MICRO-LEAK BEHAVIOR ON LMFBR MONJU STEAM GENERATOR TUBE MATERIALS

—Studies of Micro-Leak Sodium-Water Reaction (3)—

March, 1986

OARAI ENGINEERING CENTER
POWER REACTOR AND NUCLEAR FUEL DEVELOPMENT CORPORATION

動力炉・核燃料開発事業団（Power Reactor and Nuclear Fuel Development Corporation）

PNC-TN9410 86-027

Mar. 1986

MICRO-LEAK BEHAVIOR ON FBR MONJU STEAM GENERATOR TUBE MATERIALS
- Studies of Micro-Leak Sodium-Water Reaction (3) -

Mitsuo Kuroha *

Kazuhito Shimoyama *

ABSTRACT

Behavior of a micro-leak as an initiator of the leak propagation has been experimentally studied using leak nozzles made of the 2-1/4Cr-1Mo steel and Type 321 austenitic stainless steel which were selected as the heat transfer tube materials of the Monju steam generators.

Twenty-nine micro-leak tests have been carried out in three stagnant sodium pots of the SWAT-4 test rigs installed in PNC/OEC. The main test parameters were the leak rate in the range of 10^{-5} to 10^{-2} g/sec and the sodium temperature in the range of 460 to 505°C. The shapes of initial leak holes used for the tests were a circular type and a slit one.

The test results showed that the self-wastage was enhanced due to both corrosion and erosion, while the self-plugging was occurred due to precipitation of the reaction products at the sodium side and the corrsion products at the steam side. Post-test examination of the self-enlarged holes revealed that the diameters of holes were in the range of 0.3 to 0.85 mm that were insensitive to the changes in the leak rate, the material, the temperature, and the shape of the initial leak hole. The relationships among the average leak rate L_R, the self-wastage rate S_W, and the sodium temperature T was derived from the experimental data and was expressed in the form of the following equation for the above two materials.

$$S_W = \mathrm{Exp}\ (\ a\ +\ b\ \ln L_R\ -\ c\ /\ T\ )\qquad a, b, c: \text{constant}$$

---

* Plant Safety Section, Fast Reactor Safty Division, OEC/PNC

PNC-TN9410 86-027

1986 年 3 月

蒸気発生器伝熱管の微小リーク挙動試験研究

(微小リーク・ナトリウム－水反応試験研究 第3報)

黒羽 光男*・下山 一仁*

要　　旨

「もんじゅ」用蒸気発生器伝熱管材料である2－1／4 Cr－1 Mo鋼とオーステナイト系ステンレス鋼SUS 321の水リークノズルを使用して微小な水リーク領域におけるナトリウム－水反応試験を実施した。試験の目的は，これらの材料における微小リーク孔のセルフ・ウェステージによる水リーク率の拡大挙動とセルフ・プラグ時の再開口条件を明らかにするためである。

試験では，主として静止ナトリウム・ポットを有するSWAT－4装置を使用した。主要な試験パラメータは，初期水リーク率（10^{-5}～10^{-2} g／sec）およびナトリウム温度（425℃～505℃）である。ノズル孔の初期の形状は，円孔形とスリット形の二種類を選択した。

試験結果から，セルフ・ウェステージ現象およびセルフ・プラグ現象のメカニズムを解明し，材料別にセルフ・ウェステージ率および水リーク拡大率に関する実験式を導出することができ，また完全にセルフ・プラグする条件等を明確にすることが出来た。

これらの微小リークの挙動からFBR蒸気発生器での現実的な水リーク拡大シナリオにおける起因事象を理解することが出来た。また，ここで得た結果は，即応型検出系の設計条件（検出感度etc.）の決定および微小リークを検出した場合のプラント停止操作法の作成に反映することができる。

＊　大洗工学センター，安全工学部，プラント安全工学室

Contents

Page

Abstract i
Contents iii
List of Table and Figures iv
1.0 Introduction 1
2.0 Test Equipments 2
2.1 SWAT-2 2
2.2 SWAT-4 2
3.0 Micro-Leak Nozzle 3
4.0 Test Conditions and Water Injection Method 4
5.0 Test Results and Discussion 5
5.1 Outline of Micro-leak Behaviors 5
5.2 Morphology of Enlarged Hole 6
5.3 Self-Wastage Rate 7
5.4 Enlarged Orifice Diameters 9
5.5 Self-Wastage Mechanism 9
5.6 Self-Plugging 11
5.7 Self-Enlargement Time and Leak Detection Time 13
6.0 Conclusions 13
Acknowledgment 15
References 16

List of Table and Figures

Table 1. Test Conditions

Figure 1. Micro-Leak Sodium-Water Reaction Test Rig (SWAT-4)
Figure 2. Circular Type Nozzle
Figure 3. Slit Type Nozzle
Figure 4. Structure of Test Nozzle
Figure 5. Micro-Leak Behaviors (Case-1, 2)
Figure 6. Micro-Leak Behaviors (Case-3)
Figure 7. Sectional Morphorogy on Complete Self-Wasted Holes
Figure 8. Sectional Morphology on Micro-Leak Hole Progressing in Self-Wasting
Figure 9. Morphological Difference Obseved from the Sodium Side on the Self-Wastage between the Slit Type and Circular Type Nozzles
Figure 10. Self-Wastage Rates on the 2-1/4Cr-1Mo Steel
Figure 11. Self-Wastage Rates on the Austenitic Stainless Steels
Figure 12. Orifice Diameters of the Self-Enlarged Holes
Figure 13. Comparison between the Self-Wastage Rate of Type 321 Stainless Steel and Other Corrosion Data
Figure 14. Leak Enlargement Time on the 2-1/4Cr-1Mo Steel Micro-Leak Nozzle
Figure 15. Leak Enlargement Time on Type 321 Stainless Steel Micro-Leak Nozzle
Figure 16. Relation between the Leak Detection Time in the Monju Secondary Loop and the Leak Enlargement Time due to the Self-Wastage

1.0 INTRODUCTION

One distinct phenomenon of a micro-leak in an LMFBR steam generator is the self-wastage of the leak hole induced by the sodium-water reaction. It will develop into a larger one owing to complete enlargement of the leak hole, and the leak will cause the impingement wastage of adjacent tubes depending upon a diameter of the enlarged hole and a direction of the sodium-water reaction jet, so that it can trigger off a failure propagation to the adjacent tubes. On the contrary, water/steam blowdwon before the complete self-enlargement may result in blocking of the micro-hole. In this event, the difficulty of leak location will delay restarting an operation of the plant. Considering that the most of initial defects starts from a micro-leak, it is an important issue to understand the behavior of micro-leak for the design of the leak detector and shutdown systems. It is also essential to optimize an operating procedure against the micro-leak accident.

In Japan, these phenomena was first found in 1975[1)] on the water injection nozzles made of Type 304 austenitic stainless steel used for the impingement wastage tests in the small leak sodium-water reaction test loop (SWAT-2). Since the time, the preliminary tests[2)] had been conducted in SWAT-2 using thin circular nozzles made of the 2-1/4Cr-1Mo steel as simulated micro-leak holes. Later, slit-type nozzles having the same thickness as the actual heat transfer tube were used to the micro-leak behavior in the Monju steam generators. A new test rigs called SWAT-4 used exclusively for this test was constructed in 1981, and, thereafter, the test results have been accumulated.

This report presents the test results obtained in SWAT-2 and SWAT-4 together with test equipments and test procedures as follows.

- o Test Equipments
- o Micro-Leak Nozzles
- o Test Conditions and Water Injection Method
- o Test Results and Discussion

2.0 TEST EQUIPMENTS

As described, SWAT-2 was used in the early stage of the present test, then SWAT-4 used in the later stage.

2.1 SWAT-2[2)]

SWAT-2 contains approx. 200 liter flowing sodium in its main piping system. It consists of an electric heater (30 kW), an electro-magnetic pump, an electro-magnetic flow meter (max. 300 liter/min), and the test vessel (40 cm^{ID} x 2.2 m^{H}). The test vessel is equipped with a water injection system having a micro-leak nozzle. The water injection rate from the micro-leak nozzle was calculated from the change of water level in a water supply tank indicated by an eye-measurement type level gage and from the change of hydrogen concentration in sodium measured by an in-sodium hydrogen meter. A filter was installed in the water injection line, and helium gas was fed through the test nozzle to prevent its choking prior to the water injection.

2.2 SWAT-4

SWAT-4 consists of three independent stagnant sodium pots having the same geometric, and each of which connected with reaction vessel, a water injection system, a cover gas supply system, and a pressure relief system. The vessel is approx. 12 liter in its capacity, and contains 5 liter of a stagnant sodium. A layout of the test rig is shown in Figure 1. The differential pressure transmitter is connected to the water injection system, and a signal of the transmmitter is transfered to a small computer in order to record and monitor the water injection rate automatically over a long test period.

To prevent the nozzle plugging prior to a water injection, the same method as described for SWAT-2 was employed. In the test, the sodium and the cover gas in the vessel were heated at first to the specified temperature by the electric heater at the outside wall of the vessel. In the next, the feed helium gas passing through the nozzle was changed with

water. The water running through the piping in the vessel changed into steam by heating of the hot cover gas and hot sodium, and was finally superheated to the same temperature as the sodium.

During the test, the cover gas pressure inside the vessel was controlled from 0.3 to 0.6 kg/cm^2g, and the hydrogen gas generated by the sodium-water reaction was automatically released in the air through the sodium vapor trap. When the water in the injection system (approx. 80 g in capacity) was about to be consumed, additional water was fed from the reserve tank without stopping the water injection.

3.0 MICRO-LEAK NOZZLE

It is generally anticipated that a micro-defect in the heat transfer tube of the actual plant will occur in the form of a crack rather than in the circular hole, especially at the welding part. It is also seemed that the behaviors of self-plugging and self-wastage are different in the both types, and in addition, a diameter of enlarged hole depends on the original thickness, for example 0.5 mm or 3 mm.

Based on these reasons the two types of test pieces; one with a circular type defect and another with a slit one were prepared. Figures 2 and 3 show typically the circular type nozzle used in SWAT-2 and the slit one for SWAT-4, respectively. The former one was manufactured by using the spark working process, and its minimum workable diameter was approx. 90 μm when the thickness of the test pieces was near to that of the actual heat transfer tube. The latter one was manufactured by pressing a square plate with a drilled hole at the center of it. In this case each slit was constant in the length of approx. 0.5 mm, so that the equivalent diameters of leak holes were manufactured in the range of 10 to 100 μm by controlling their widths. Figure 4 shows a total structure of the slit type test piece and its attachment.

The equivalent diameter of the slit type hole was estimated by the known experimental formula and by measuring the time when it took for

argon to discharge through the slit from the small tank to the atmosphere until the pressure in the tank reduced from a certain value to another one. The formula was beforehand derived from the discharging times of argon through the circular holes in the above same apparatus.

4.0 TEST CONDITIONS AND WATER INJECTION METHOD

Table 1 shows the test conditions for SWAT-2 and SWAT-4. The sodium temperatures and the steam pressures in the table are selected according to the operating conditions of the Monju steam generators. The materials of test pieces were either the 2-1/4Cr-1Mo or Type 321 austenitic stainless steels, that were selected for the heat transfer tubes of the Monju steam generators. The design sepicification of the Monju steam generators are as follows:

	Materials, Thickness of tube wall	Sodium inlet temperature (°C)	Steam outlet temperature (°C)	Steam outlet pressure (kg/cm^2g)
Evaporator	2-1/4Cr-1Mo, 3.8 mm	455.6 - 469.3	369	129.8 - 145.7
Superheater	Type 321 SS, 3.5 mm	489.5 - 505	487	128.5 - 133

The conditions such as the sodium and steam flow conditions, the sodium pressure, the steam temperature, and the sodium impurity shown in Table 1 are different from those for the plant conditions. Fortunately, these values are supposed to be negligible effect for the test results. The equivalent diameters of the test nozzles were selected to obtain such a range of the micro-leak rates that does not cause the impingment wastage of adjacent heat transfer tubes.

The test was started by operating the two valves to change the helium gas supply line to the water injection one. When the leak rate developed into larger one owing to the complete self-enlargement of leak hole and output of the water level gage decreased from initial 5 to 1.2 volts, the water injection automatically finished by closing a valve in the water injection line. At the same time, the pressurized helium and water/steam were released to the atmosphere.

After the water injection test, the sodium and the reaction products mixture was vacuumed out of the test vessel. The test nozzle was removed, and was cleaned with steam for inspections.

5.0 TEST RESULTS AND DISCUSSION

Eighteen 2-1/4Cr-1Mo steel nozzles (six circular and twelve slit type ones) and eleven Type 321 stainless steel nozzles (all slit type ones) were used for this test. The followings are the detailed results and discussion.

5.1 General Description of Micro-Leak Behaviors

Micro-leak behaviors observed in the tests can be classified into the following three cases.

Case 1: In the initial leak rates of more than 10^{-2} g/sec, the leak rate is kept comparatively constant as shown in Figure 5(a) for either material, and consequently develops rapidly owing to the self-wastage penetration.

Case 2: In the cases of the leak rate less than 10^{-2} g/sec, it reduces for the short period to the range of 10^{-4} to 10^{-5} g/sec. In such cases of the 2-1/4Cr-1Mo steel nozzle, the leak rate frequently reduces further with time to approx. 10^{-7} g/sec owing to the self-plugging in the leak hole. This leak rate is kept for the long period, and it almost never returns to

the initial value with a few exception as shown in Figure 6(a).

Case 3: Contrary to Case 2, the micro hole does not choke completely even at the leak rate as small as less than 10^{-4} g/sec, and the reduced leak rate finally returns to a level of the initial one, and results to develop rapidly as shown in Figure 6(b). Generally, it takes approx. ten minutes for the leak rate at final stage to increase from 10^{-3} to 10^{-2} g/sec, and with additional 30 seconds the value reaches its maximum.

The water injection rates measured by the water level gage indicated larger values more than the actual ones in the leak rates of more than 1 g/sec, because the steam change into hot water with increasement of leak rates. Therefore, the maximum leak rates in Figures 5(a), 6(a), and 6(b) are only referencial values. Thus, after cleaning of the nozzles, each accurate value was estimated by measuring the equivalent diameter of the enlarged one by the same method as described in Chapter 3.

5.2 Morphology of Enlarged Hole

Figures 7 (a) and (b) show sections of the complete enlarged holes, which are typical examples of the 2-1/4Cr-1Mo steel at sodium temperature of 470°C and Type 321 stainless steel at 505°C, respectively. There are slight differences in the self-wasted shapes between the both. The shapes observed in the tests are generally paraboloid or conical with openings toward the sodium side, in which maximum diameters are almost 2 to 3 mm. They are rare in the cylindrical and hemispherical shapes.

Interruption of the water injection on the way of self-wastaging leaves the through slit original on the steam side, while the slit is wasted on the sodium side and the original shape is not retained at all as shown in Figure 8. These results indicate that the enlargement of the nozzle inner diameter first occurs at the sodium side, then proceeds to the water side through the nozzle center, and when it reaches the steam side the leak rate increases dramatically.

In the average leak rate before the complete self-enlargement of less than 10^{-3} g/sec, the metal around the enlarged hole of the 2-1/4Cr-1Mo steel is corroded on the sodium side by a thickness of approx. 0.2 mm as shown in Figure 7 (a). In the average leak rate of less than 10^{-5} g/sec, the test period grows more than a few days, so that oxidation of the steam side is generated in large quantities. In the case like Figure 6 (b), a large reduction in thickness around the enlarged hole in the oxide layer of the steam side was found. On the other hand, in case of the stainless steel nozzles, they did not occur on the steam side at all because of small oxidation in the steam side, though slight reduction in thickness occurred on the sodium side in the leak rates of less than 10^{-4} g/sec and the sodium temperature of 505°C as shown in Figure 7(b).

Figures 9(a) and (b) show two different morphologies observed from the sodium sides of the enlarged nozzles made of the 2-1/4Cr-1Mo steel, which are typical examples of the circular and slit type nozzles, respectively. The feature of these morphologies is that the only two sides of the slit hole were remarkably self-wasted, while the surroundings of the circular hole was uniformly self-wasted. A reason that causes these different morphologies seems to be that the ways of the steam injection through the leak holes are different by the geometric shape of the nozzles like the slit or circular ones. This also indicates that the errosive effect by the steam flow exist as one of the mechanism of self-wastage.

5.3 Self-wastage Rate

Figures 10 and 11 show the self-wastage rates of the 2-1/4Cr-1Mo and Type 321 stainless steels, respectively. The relationship among the average leak rate, L_R (g/sec), the sodium temperature, T (°K), and the self-wastage rate, S_W (mm/sec), which means the penetration rate of leak hole, are obtained as follows:

2-1/2Cr-1Mo Steel

slit type:

$$S_W = \mathrm{Exp}\ (\ 46.2 + 0.82\ \ln L_R - 36{,}890\ /\ T\ ) \quad \cdots\cdots\cdots\cdots \quad (1)$$

$(L_R = 10^{-5} - 10^{-1}\ g/s)$

$(T = 460 - 482°C)$

circular type:

$$S_W = \mathrm{Exp}\ (\ -4.06 + 0.58\ \ln L_R\ ) \quad \cdots\cdots\cdots\cdots\cdots\cdots\cdots \quad (2)$$

$(L_R = 10^{-5} - 10^{-1}\ g/s)$

$(T = 472 - 490°C)$

Type 321 Stainless Steel

slit type:

$$S_W = \mathrm{Exp}\ (\ 11.07 + \ln L_R - 10{,}420\ /\ T\ ) \quad \cdots\cdots\cdots\cdots \quad (3)$$

$(L_R = 10^{-5} - 10^{-1}\ g/s)$

$(T = 425 - 505°C)$

These equations were derived by assuming that the temperature effect varies according to an Arrhenius' law. The GE's data[4] are refered to the temperature dependence of the above equation (1). The tests using the circular type nozzles of the 2-1/4Cr-1Mo steel produced similar results to the GE's data. However, the self-wastage rates of the slit ones are overall less than that of the circular ones, particularly in the smaller leak rates. This appears to be explained as follows by a difference in the configuration between the both nozzles: namely, A slit length "s" of the slit hole manufactured is almost constant regardless of a variaty of equivalent diameters, while a circumference "c" of the circular hole depends on the diameter, so the value of "s/c" increases in inverse proportion to the diameter of circular hole. Consequently, the sodium-water reaction per unit length around the leak hole becomes milder in the slit type nozzle than in the circular one at the same leak rate.

Equations (1) and (3) indicate that the 2-1/4Cr-1Mo steel has a

remarkable dependency of temperature for the self-wastage rate comparing Type 321 stainless steel, and the latter one has a greater dependency of leak rate.

Compared to the GE's test of Type 316 stainless steel, Type 321 stainless steel in the tests has lower resistance to self-wastage than Type 316 one.

The austenitic stainless steel has also a greater resistance to the self-wastage than the 2-1/4Cr-1Mo one. This reason is because there is a large difference in the content of chromium and nickel, which are well known as high resistant materials against the impingement wastage by the sodium-water reaction and corrsion by aqueous solution of sodium hydroxide.

5.4 Enlarged Orifice Diameters

Figure 12 shows the relation between the average leak rate before the complete self-enlargement and the orifice diameters in the enlarged holes. These orifice diameters are in a range of 0.3 to 0.85 mm, with no relations to the average leak rates, the materials, the temperatures, and the initial nozzle shapes. Therefore, the developing ratio in the leak rate tends to increase as the average leak rate decreases.

If these orifices are made in the heat transfer tube of the Monju steam generator, the leak rate will be 1 to 9 g/sec at the outlet of the superheater and 2 to 12 g/sec at the one of the evaporator. Because the impingement of wastage of adjacent tubes is most easy to occur in these leak rates, it is necessary to develop a fast response type leak detector like an acoustic one. If the detection sensitivity could be ideally reduced to 1 g/sec with the fast blowout of water/steam, it would minimize more damaged adjacent tubes.

5.5 Self-wastage Mechanism

On the base of Figure 8, the concentration of the sodium-water reaction products seems to be a strong parameter of the self-wastage.

The corrosion rate of the 2-1/4Cr-1Mo steel by 100% solution of NaOH (400 - 500°C) is approx. 8×10^{-7} mm/sec[5]. This low value indicates that even if the concentration of NaOH is very high, it only is not sufficient to explain the self-wastage phenomenon.

The following chemical reactions are assumed for the mechanisum of accelerative corrosion:

Solution side:	$Na(\ell) + H_2O(\ell) \longrightarrow NaOH(\ell) + 1/2H_2(g)$	.. (4)
mainly consists of NaOH and Na_2O	$2NaOH(\ell) \longrightarrow Na_2O(\ell) + 1/2H_2(g)$	.. (5)
Metal side:	$M(s) + 2Na_2O(\ell) \longrightarrow NaMO_2(\ell) + 3Na(\ell)$	.. (6)
metal oxides are formed	(M; Fe, Cr, Ni, Mo)	

C.F. Knights et al. paied attention to the corrosion effect of the Na_2O concentration (X) in NaOH and reported that the corrosion rate was proportional to $Exp(1.3\ X^{0.5})$ in the 2-1/4Cr-1Mo steel[6]. Figure 13[6] shows comparison of corrosion rates of 2-1/4Cr-1Mo, 9Cr-1Mo and Type 316 stainless steel discs spinning at 6000 rpm in Na_2O-NaOH melts. They concluded that the enhancement of corrosion by Na_2O additions to NaOH melt arises from an enhancement of the solubility of the corrosion products as shown in the below table.

Solubility of $NaFeO_2$ and $NaCrO_2$ in Hydroxide Melts at 750°C

Compound \ Melt	NaOH $^{w}/_{o}$		NaOH-40$^{w}/_{o}$ Na_2O	
$NaFeO_2$	2.32	2.07	15.6	17.4
$NaCrO_2$	0.006	0.004	0.45	0.55

In the case of the sodium-water reaction, the concentration of Na_2O is determined by the generation rate (dependent on the leak rate) and the disintegration rate (dependent on the temperature) of NaOH. The concentrations of these compounds at the leak position increase as the leak rate is larger and the temperature is higher, which increase the self-wastage rate as shown in Figure 13. This figure shows that the self-wastage rates of Type 321 stainless steel in the micro-leak rates of 10^{-7} to 10^{-6} g/sec are approximately equivalent to the corrosion rate of pure NaOH, and that of 10^{-4} to 10^{-2} g/sec are equivalent to that of $70^{w}/o$ Na_2O addition to NaOH melt.

It is also found that there is the errosive effect owing to the steam flow as shown in Figure 9. This steam flow removes the above corrosion products and continuously provides a new corrosion surface to promote the reactions like the impingement wastage.

The effect of temperature on self-wastage is much greater than that obtained from the general corrosion tests using high sodium temperature or high sodium hydoxide temperature. The reason seems to be because the generating rates of Na_2O and $NaMO_2$ are greatly affected by temperature. The self-wastage rate of Type 321 stainless steel had a smaller temperature dependence on the self-wastage rate because it has a better oxidation resistance and the $NaMO_2$ formation rate is assumed to be lower.

5.6 Self-plugging

Figure 14 indicates the self-enlargement time of the slit type 2-1/4Cr-1Mo steel nozzles. The abscisa is the equivalent diameter of the slit type nozzle measured prior to the test. The test marked with an arrow was stopped before the complete enlargement owing to the self-wastage because the leak rate was reduced less than 10^{-6} g/sec and the nozzle seemed to be perfectly choked. The broken line in the figure shows the complete enlargement time of the through slit of 3.8 mm thickness which was estimated by the above equation (1) assuming no plugging of the leak hole. The figure shows that the leak slits seem to be perfectly choked for the equivalent diameters less than 70 μm and the width less

than 12 μm. The slits are almost choked in the equivalent diameters of 70 to 85 μm, which therefore, need the self-enlargement times of several hours to several days. For 85 μm or more, the ratio of the partial plugging ratio is approx. 30%.

Figure 15 shows the relationship between the equivalent diameters of the initial leak slits and the self-enlargement times on Type 321 stainless steel nozzles in the same way as Figure 14. This figure shows that although these nozzles tend to have partial clogging, complete chockes occur in the very rare cases. However, the possibility of complete plugging will increase in the equivalent diameters of less than 30 μm (less than 5 μm in width).

As mentioned above, the self-plugging behavior on the 2-1/4Cr-1Mo steel nozzles are different from those of Type 321 stainless steel ones. Because the latter has a greater resistance to steam oxidization, the oxidized scale layer is thinner. This is considered to be the reason why the stainless steel nozzles are not easily plugged even if the slit width is small. Generally, the growth speed, y (μm), of the scale in high temperature steam is expressed as a function of time t (hour) as follows:

$$y = kt^{1/2} \qquad \cdots\cdots\cdots\cdots\cdots \quad (7)$$

From this test results, the speed constant k for Type 321 stainless steel was calculated to be approx. 0.15 on the base of the complete plugging time of the slit hole and its initial width. A measured value k was 0.2 in the case of Type 304 stainless steel of a sodium heated steam generator which was operated for approx. 40 days[7]. It is nearly equal to the above value. Likewise, k for that of the 2-1/4Cr-1Mo steel was also calculated to be approx. 0.9. Once plugged, neither a steam blow nor a thermal shock remedy was successful in reopening it regardless of material. On the other hand, a reason that there is a large scattering in data on the self-enlargement times in Figures 14 and 15 is that the initial partial plugging caused by the sodium-water reaction products at the nozzle outlet is different from case to case.

5.7 Self-Enlargement Time and Leak Detection Time

Figure 16 shows a relation between the leak enlargement time due to the self-wastage and the small water leak detection time in the Monju secondary loop. The detection times in the figure were estimated by the SWAC-10 code[8], and the leak less than 10^{-1} g/sec will be detected by the in-sodium hydrogen meters with two kinds of alarm level, level high (① curve in Figure 16), ROR high (② curve). The curves ④ and ⑤ in the figure are the self-enlargement times at the upper part of the Monju evaporator and the one of the super-heater, respectively, and were estimated by the experimental equations (1) and (2) obtained by this tests.

This figure indicates that the in-sodium hydrogen meters can detect the leak in the range of 10^{-3} - 10^{-1} g/sec before the complete self-enlargement of a micro-leak, however, the operators in Monju are required to decide rapidly whether the alarm is spurious or not, because these alarm levels are not an initiator of the automatic water/ steam blowdwon.

6.0 CONCLUSIONS

As mentioned in the preceeding chapters, data on micro-leak behavior have been obtained with regard to the 2-1/4Cr-1Mo steel and Type 321 austenitic stainless one.

The data are briefly summarized as follows.

(1) The dominant mechanism of the self-wastage is a co-operation between the corrosive effect by the sodium-water reaction products like NaOH and Na_2O and the erosive one by the steam flow like the impingement wastage.

(2) The relationship among the average leak rate, L_R (g/sec), the self-wastage rate, S_W (mm/sec), and sodium temperature, T (°K), are as follows for the slit type nozzle:

2-1/4Cr-1Mo steel;

slit type

$$S_W = \mathrm{Exp}\ (\ 46.2 + 0.82\ \ln L_R - 36{,}890/T\ )$$

$(L_R = 10^{-5} - 10^{-1}$ g/s)

(T = 460 - 482°C)

circular type

$$S_W = \mathrm{Exp}\ (\ -4.06 + 0.58\ \ln L_R\ )$$

$(L_R = 10^{-5} - 10^{-1}$ g/s)

(T = 472 - 490°C)

321 stainless steel;

slit type

$$S_W = \mathrm{Exp}\ (\ 11.07 + \ln L_R - 10{,}420/T\ )$$

$(L_R = 10^{-5} - 10^{-1}$ g/s)

(T = 425 - 505°C)

(2) Most outlines of the self-wasted nozzles are like a cone shape which open to the sodium side. All orifices after the complete self-enlargement are formed near the steam side. The orifice diameters are found to be in the range of 0.3 to 0.85 mm without being significantly influenced by the average leak rates, the materials, the temperatures, and the nozzle shapes.

(3) For a initial leak rate of 10^{-2} g/sec or less, partial plugging of the leak hole is likely to be caused by the sodium-water reaction products regardless of the materials, and the leak rate tend to decrease to 10^{-3} g/sec or lower.

(4) In the above case, because Type 321 austenitic stainless steel has a higher resistance to steam corrosion than the 2-1/4Cr-1Mo steel, the leak hole of the former is unlikely to become completely plugged when its equivalent diameter is more than 30 μm. The probability of the complete self-enlargement of the 321

stainless steel is, therefore, ultimately larger than that of the 2-1/4Cr-1Mo steel. On the 2-1/4Cr-1Mo steel nozzle, the complete plugging will almost take place in the equivalent diameters of less than approx. 70 μm.

It is our intention in the future to collect relevant data on micro-leak behavior of high chromium and alloy steels which are proposed as materials in the heat transfer tubes of future large scale steam generators.

Acknowledgment

The authors wish to express their gratitude to Dr. Y. Himeno for helpful suggestion and essential comments on this study, and for his editorial check of the final report.

REFERENCES

1) N. Kanegae, et al.," Wastage and Self-Wastage Phenomena Resulting from Small Leak Sodium-Water Reaction - Studies of Small-Water Reactions (7) -," PNC SN941 76-27, March 1976.

2) M. Kuroha, et al.," Preliminary Study of Micro-Defect Self-Wastage on 2-1/4 Cr-1Mo Steel Nozzles for LMFBR Steam Generators - Studies of MicroLeak Sodium-Water Reactions (1) -," PNC SN941 80-135, Jun. 1980.

3) M. Kuroha, et al.," Study of Micro-Defect Self-Wastage Phenomena on LMFBR Prototype Steam Generators - Studies of Micro-Leak Sodium-Water Reactions (2)-," PNC ZN941 82-101, April 1982.

4) J.A. Gudahl, P.M. Magee,"Microleak Wastage Taste Results," GEFR-00352, March 1978.

5) Y. Sakumoto, et al.," Corrsion Behaviours of Materials for Steam Generator in the Contaminated High Temteparature Sodium," PNC SJ222 84-08, June 1984.

6) C.F. Knights, R. Perkins," Corrosion of Steel by the Molten Products of the Na/H_2O Reaction," AERE Harwell, August 1979.

7) M. Kuroha, T. Sasaki et al.," Material Examination of Steam Generator Tubes," PNC SN941 77-175, November 1977.

8) O. Watanabe, M. Kishida, et al., "User's Manual of Safety Map Code SWAC-10-MJ/2 - Evaluation Detector Capability against Small Leak Sodium-Water Reaction -," PNC SJ906 79-02, December 1979.

Table 1 Test Conditions

	SWAT-2	SWAT-4
Sodium Temperature (°C)	approx. 480	505*, 470, 460*, 425*
Steam Pressure (kg/cm^2g)	40 100	130
Oxygen Content in Sodium prior to Test (ppm)	< 10	< 100
Sodium Flow Velocity (cm/sec)	approx. 8	0
Cover-Gas Pressure (kg/cm^2g)	0.5	0.4 0.5
Nozzle Material	2-1/4Cr-1Mo	2-1/4Cr-1Mo, Type 321SS
Nozzle Type	Circular	Slit
Nozzle Thickness (mm)	0.5 3.6	3.8, 3.5*
Equivalent Diameter of Nozzle (mm)	40 250	46 90, 22* 96*

note: A mark * shows the value adopted for Type 321SS nozzle.

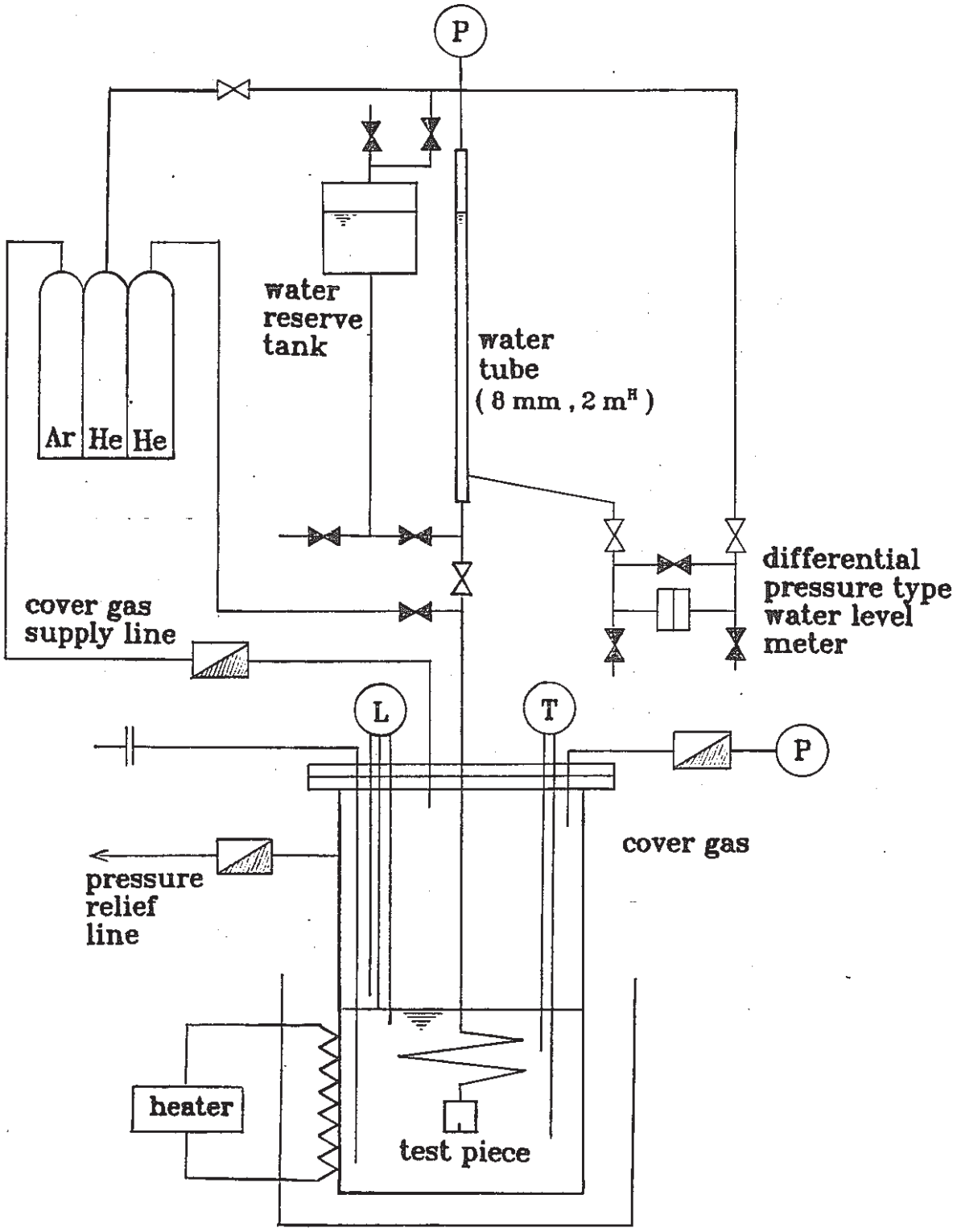

Figure 1 Micro-leak Sodium-water reaction test rig (SWAT-4)

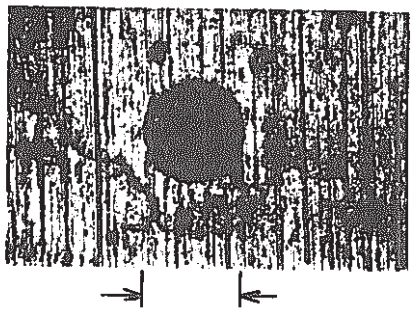

(a) Surface

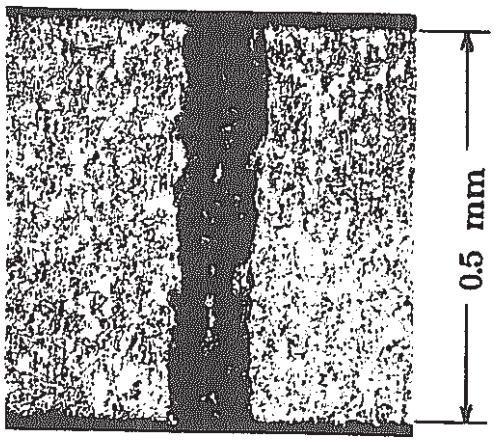

(b) Section

Figure 2 Circular type nozzle

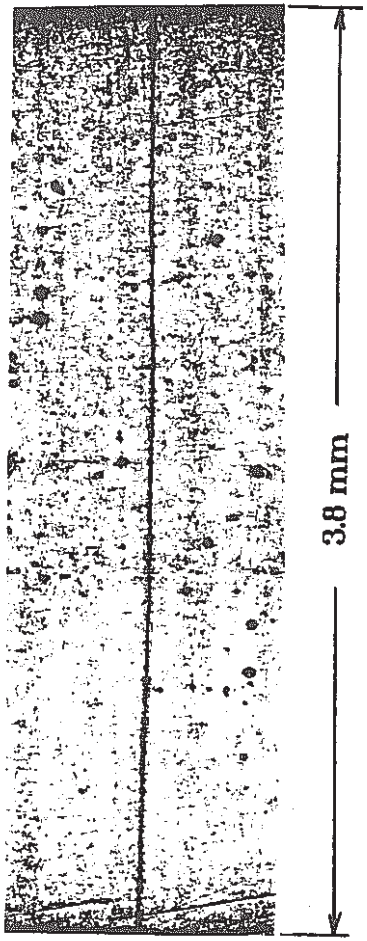

(a) Section

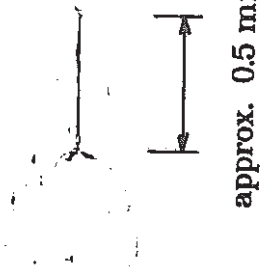

(b) Front Surface

(c) Back Surface

Figure 3 Slit Type nozzle

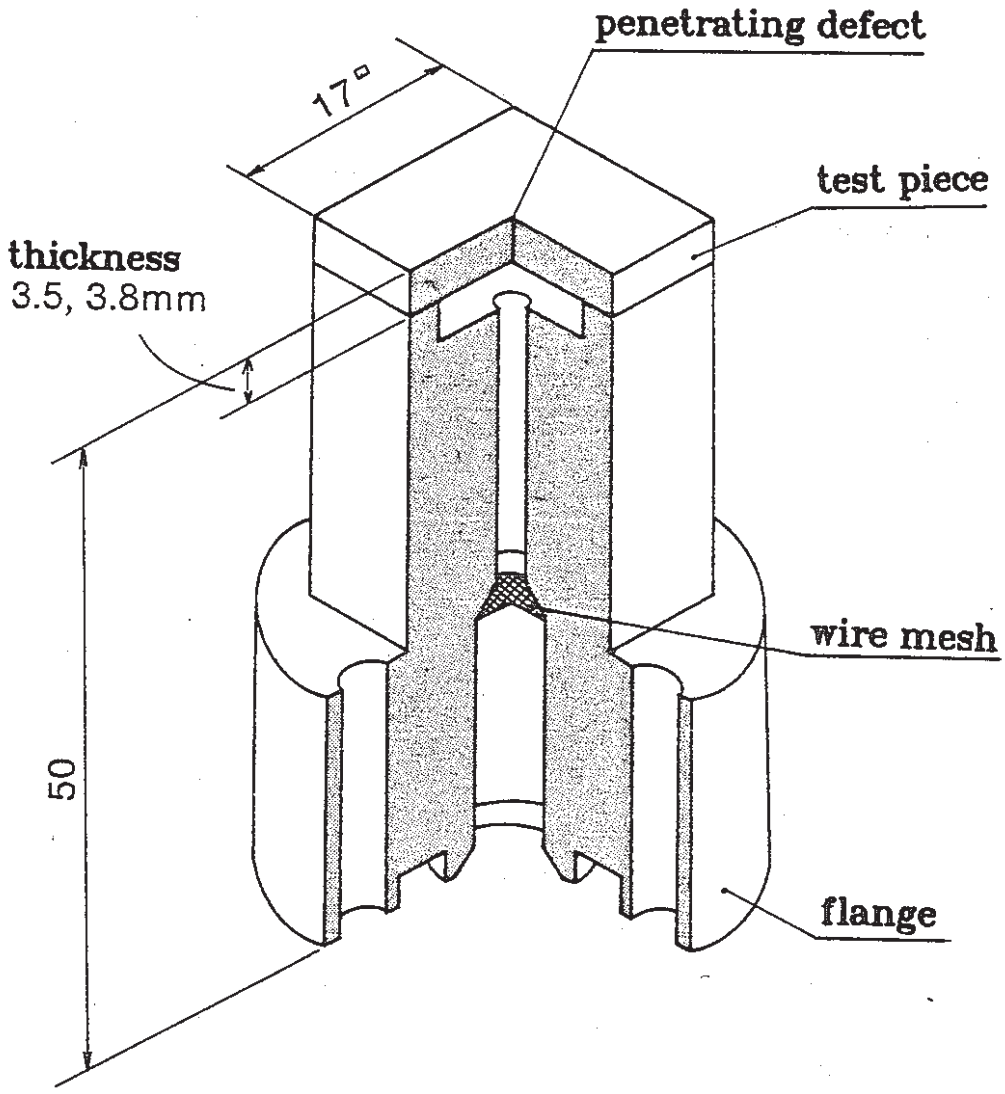

Figure 4 Structure of test nozzle

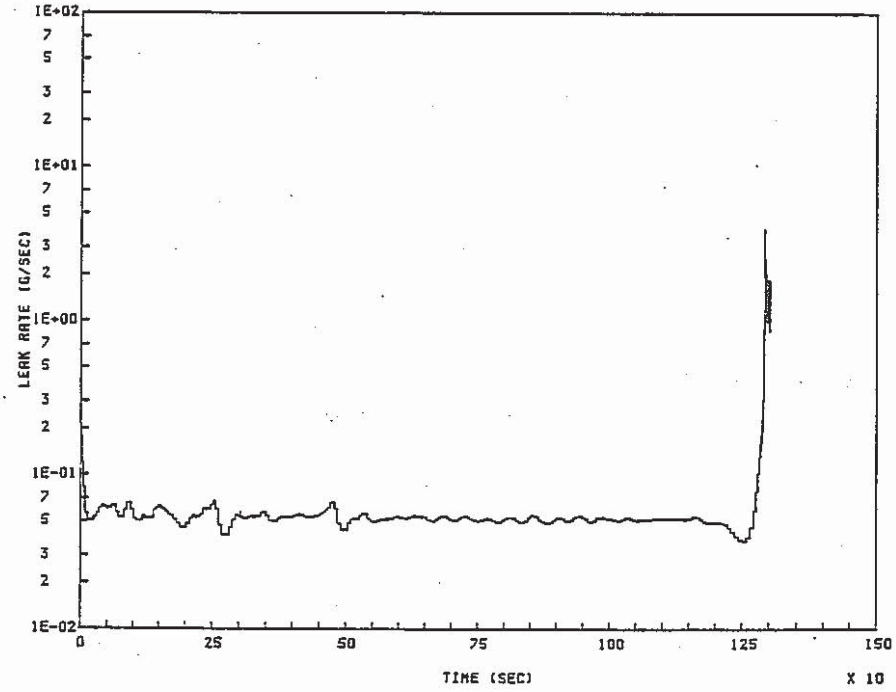

(a) 2-1/4Cr-1Mo Steel, 470 °C (Case-1)

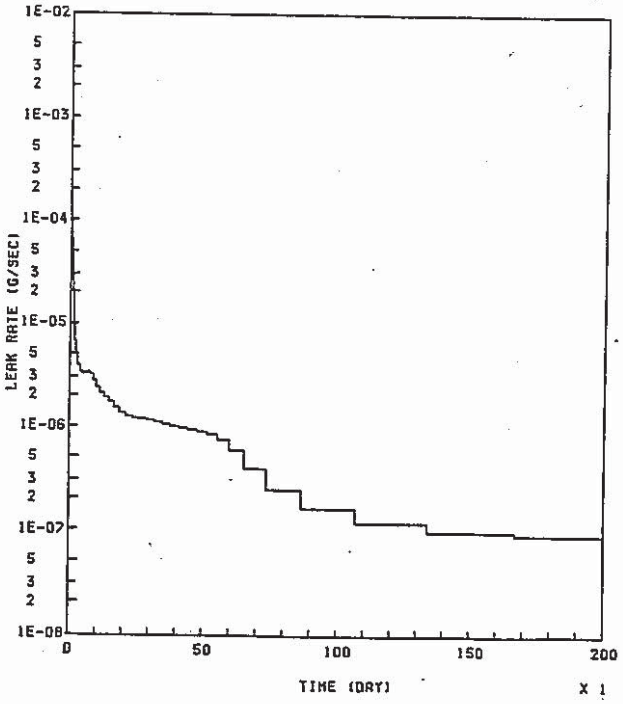

(b) 2-1/4Cr-1Mo Steel, 470 °C (Case-2)

Figure 5 Micro-leak behaviors (case-1,2)

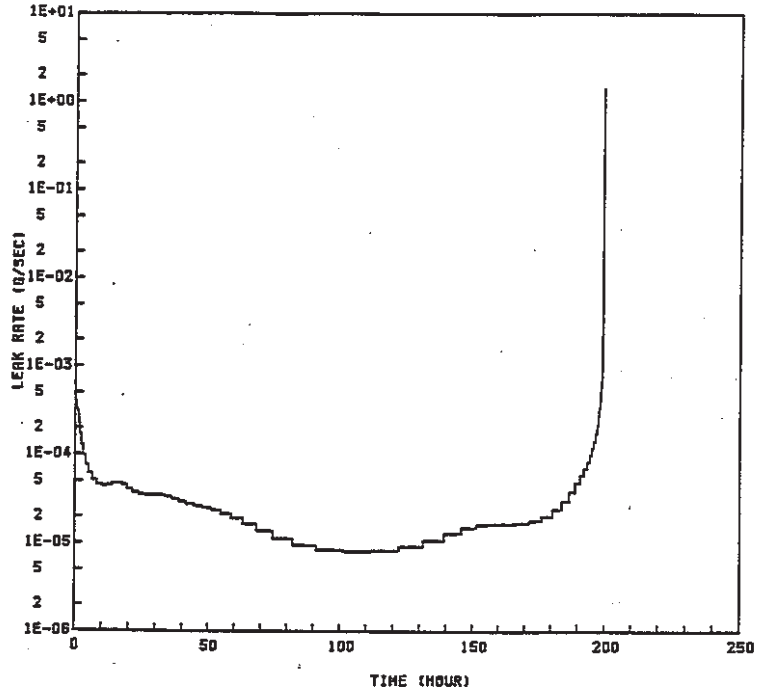

(a) 2-1/4Cr-1Mo Steel, 470 °C (rare case)

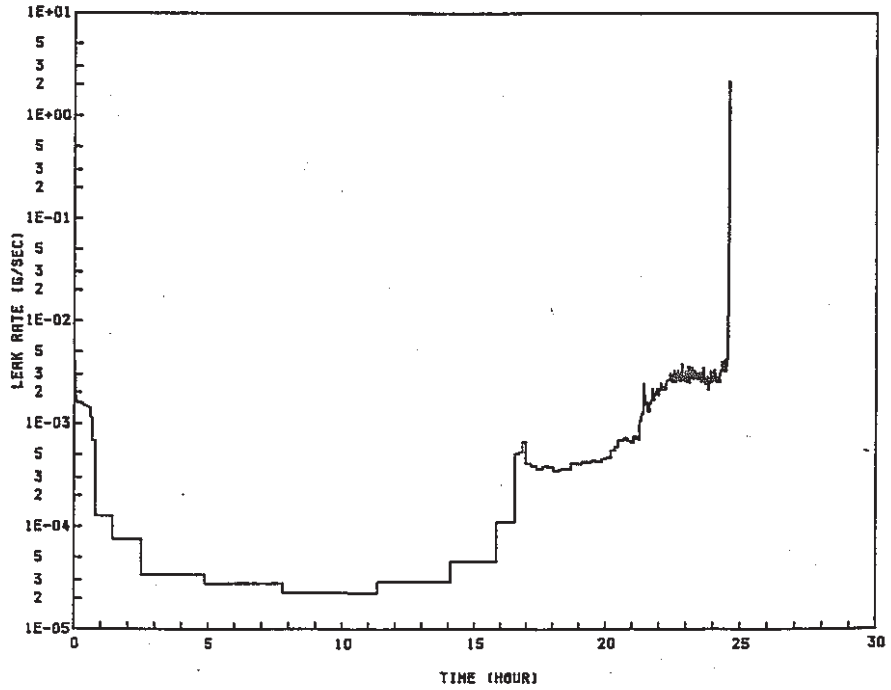

(b) 321 Stainless Steel, 505 °C

Figure 6 Micro-leak behaviors (case-3)

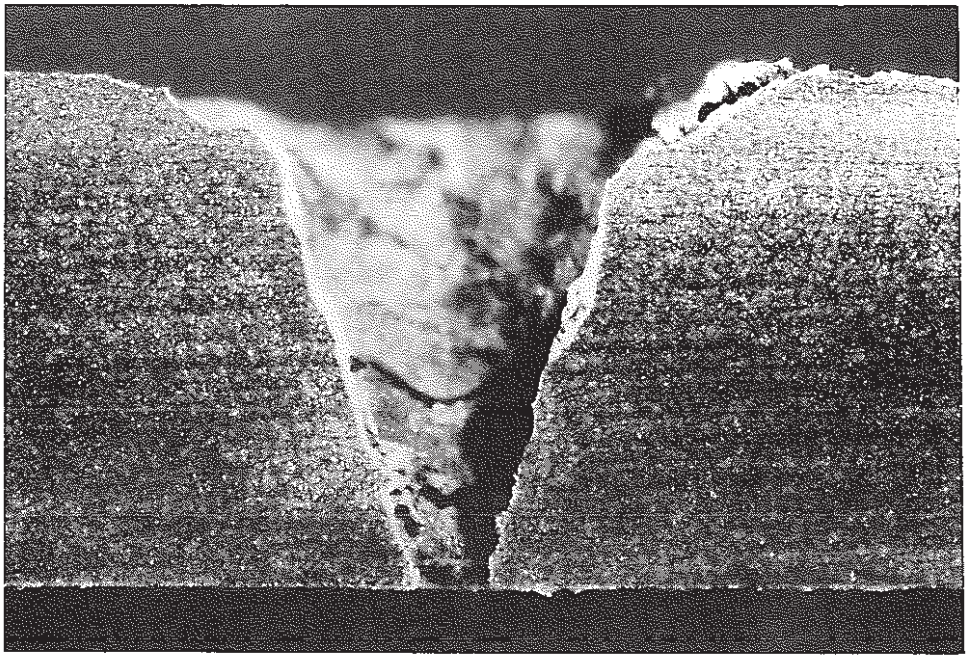

(a) 2-1/4Cr-1Mo Steel
Average leak rate : 5×10^{-4} g/sec
Self-wastage rate : 3×10^{-5} mm/sec
Sodium temp. : 470 °C

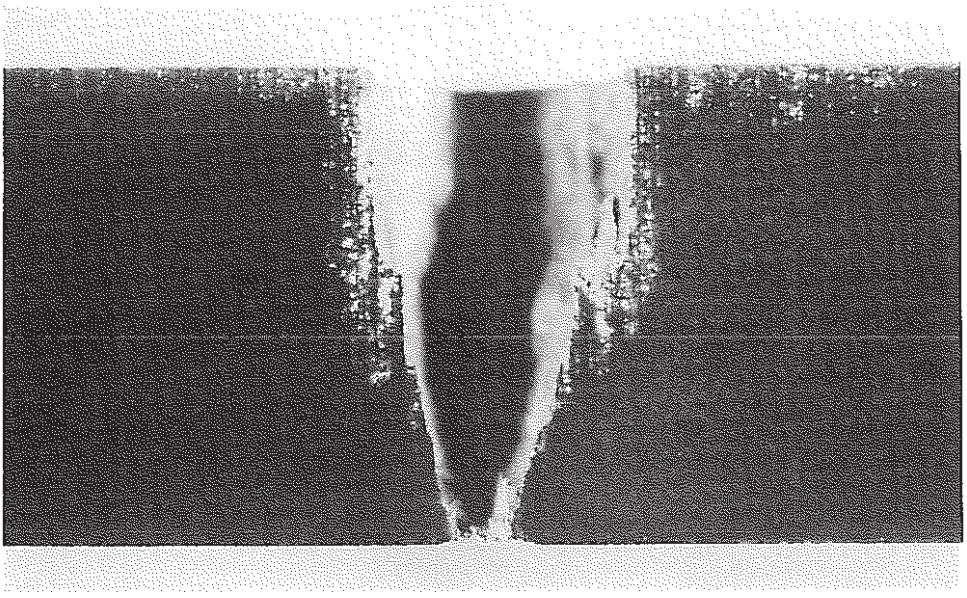

(b) 321 Stainless Steel
Average leak rate : 8×10^{-5} g/sec
Self-wastage rate : 4×10^{-6} mm/sec
Sodium temp. : 460 °C

1 mm

Figure 7 Sectional morphology on complete self-wasted holes

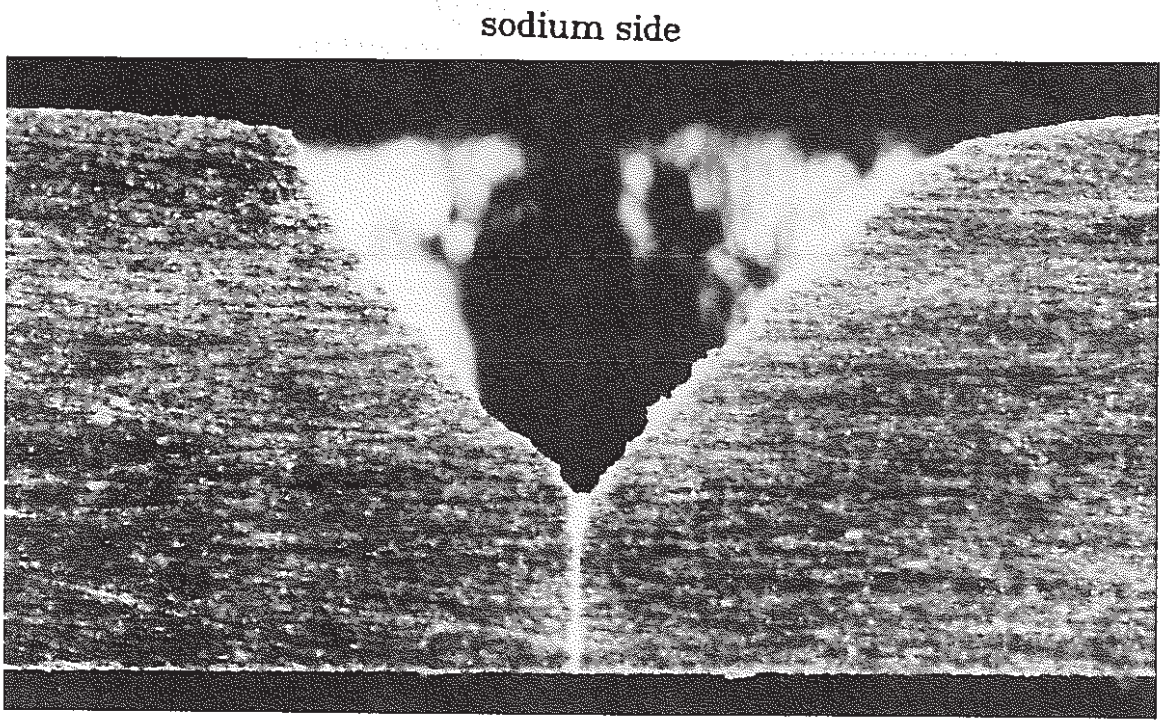

Figure 8 Sectional morphology on micro-leak hole progressing in self-wasting

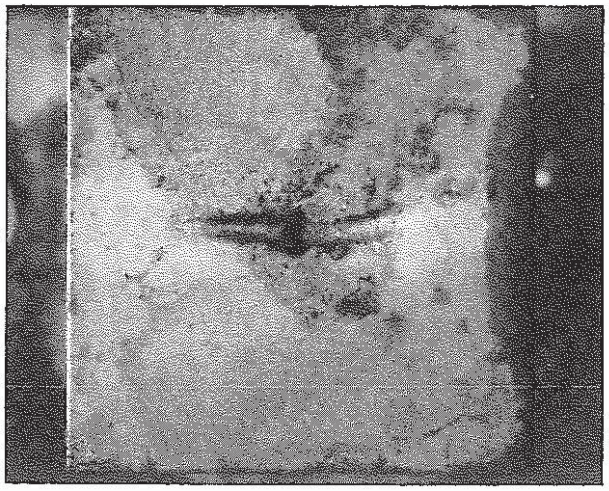

- Equivalent diameter of initial leak hole = 92 μm
- Average leak rate = 8×10^{-2}
- Sodium temperature = 400 °C
- Steam injection time = 55 min.

(a) Slit Type Nozzle (2-1/4Cr-1Mo)

5 mm

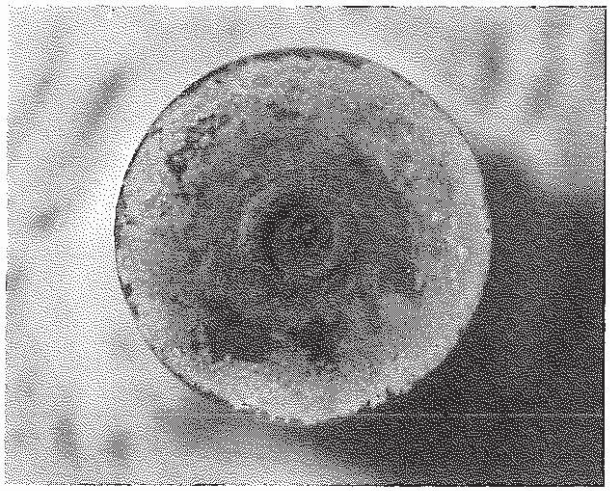

- Equivalent diameter of initial leak hole = 90 μm
- Average leak rate = 3.2×10^{-2} g/sec
- Sodium temperature = 480 °C
- Steam injection time = 20 min.

(b) Circular Type Nozzle (2-1/4Cr-1Mo)

Figure 9 Morphological difference observed from the sodium side on the self-wastage between the slit type and circular type nozzles

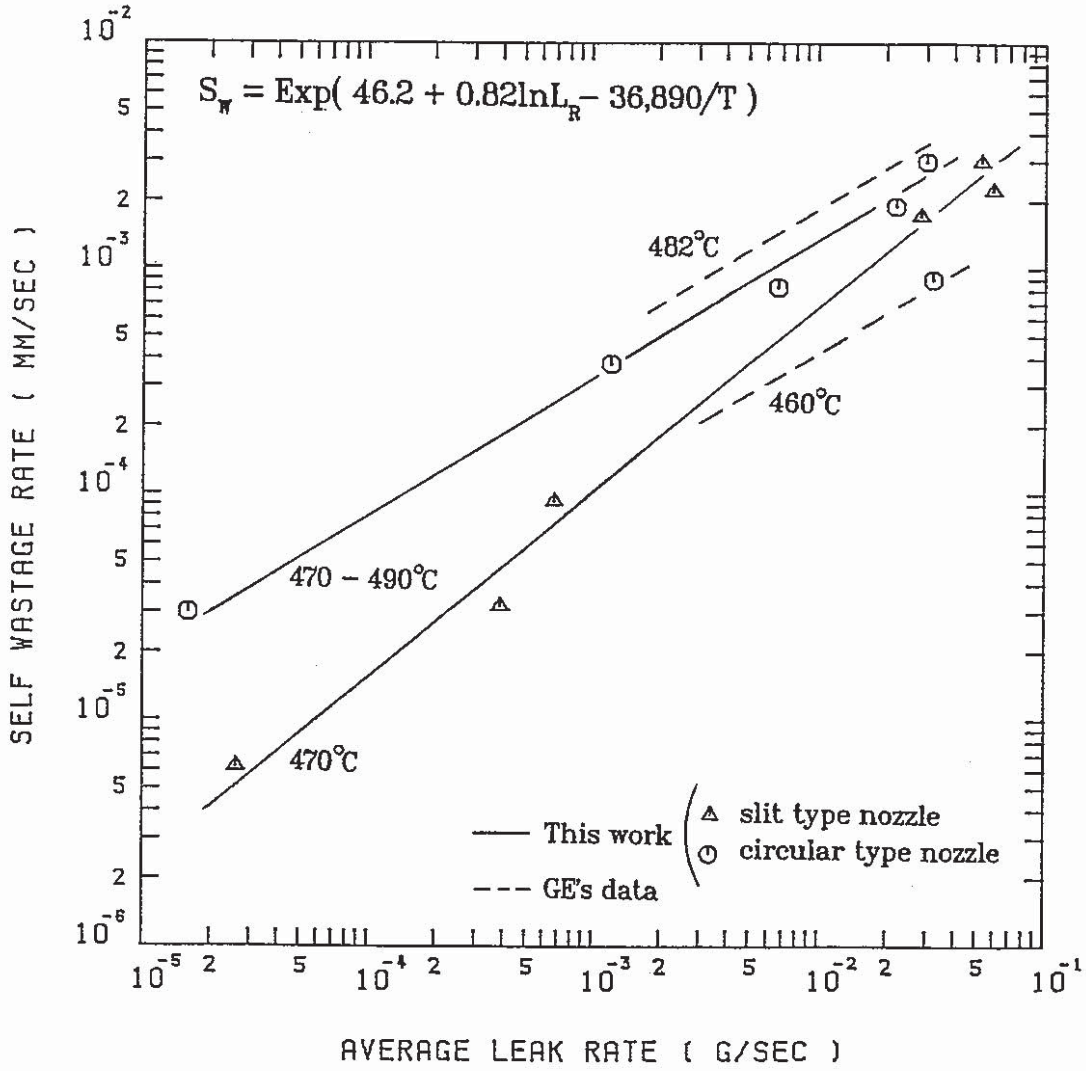

Figure 10 Self-wastage rates on the 2-1/4Cr-1Mo steel

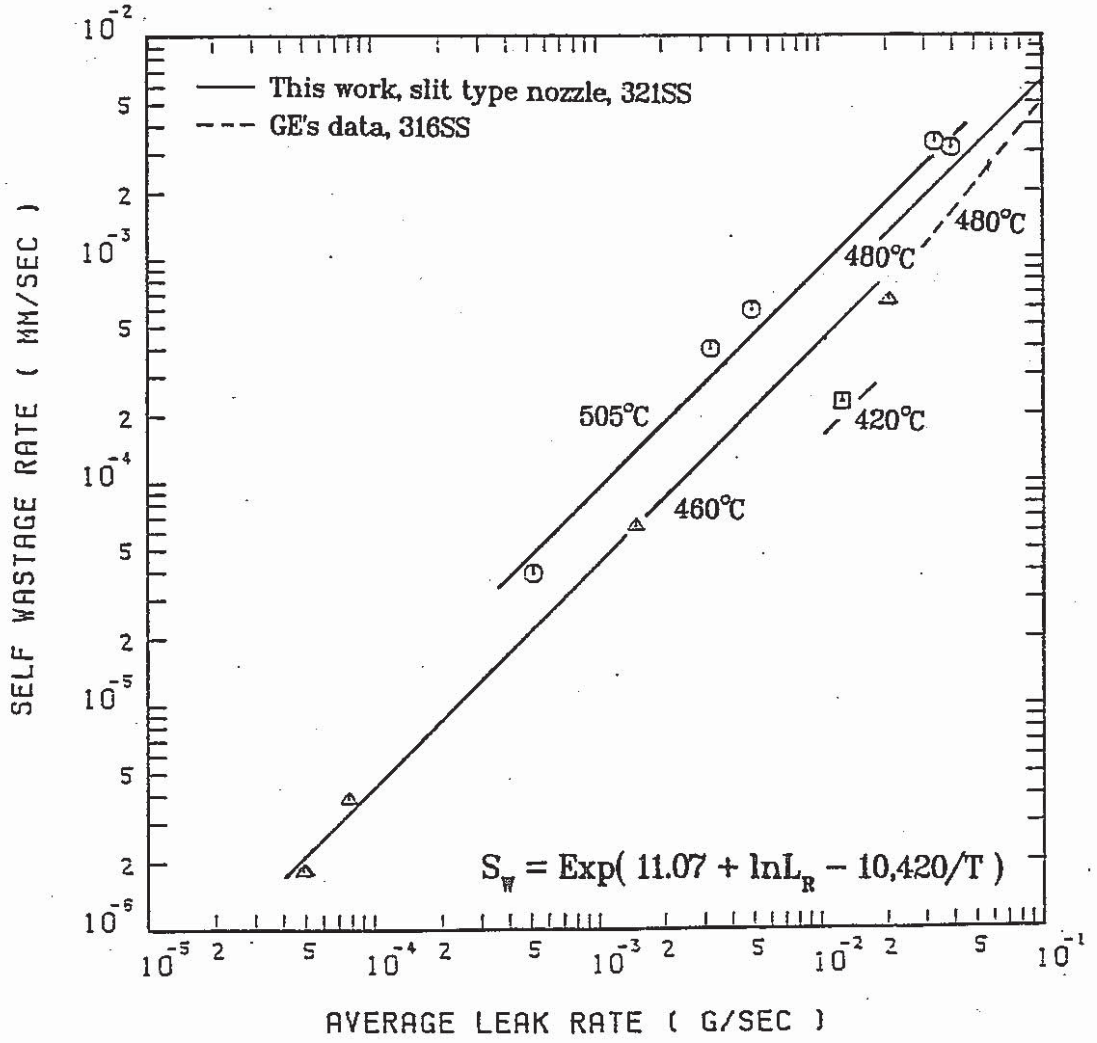

Figure 11 Self-wastage rates on the Austenitic stainless steels

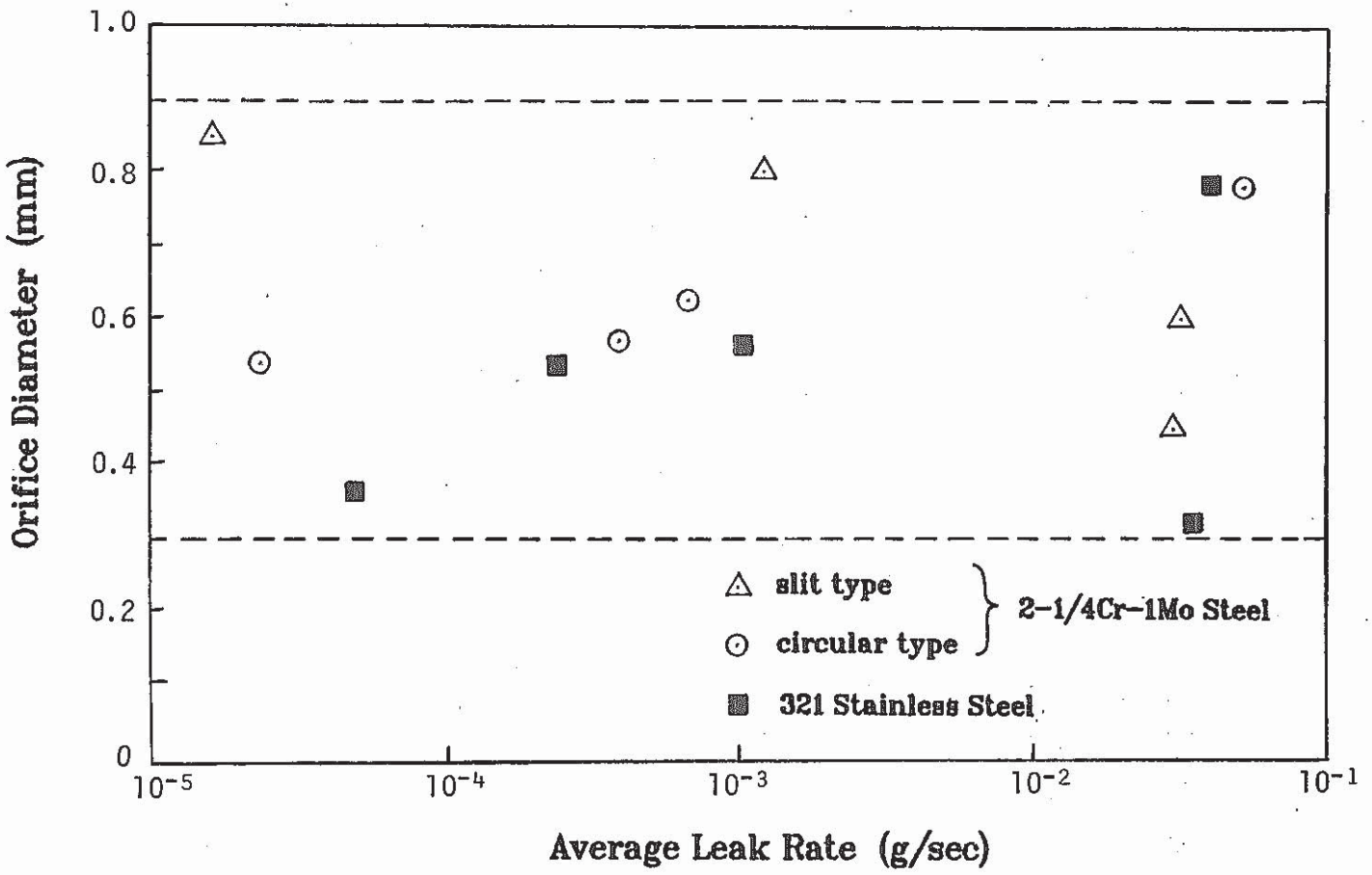

Figure 12 Orifice diameters of the self-enlarged holes

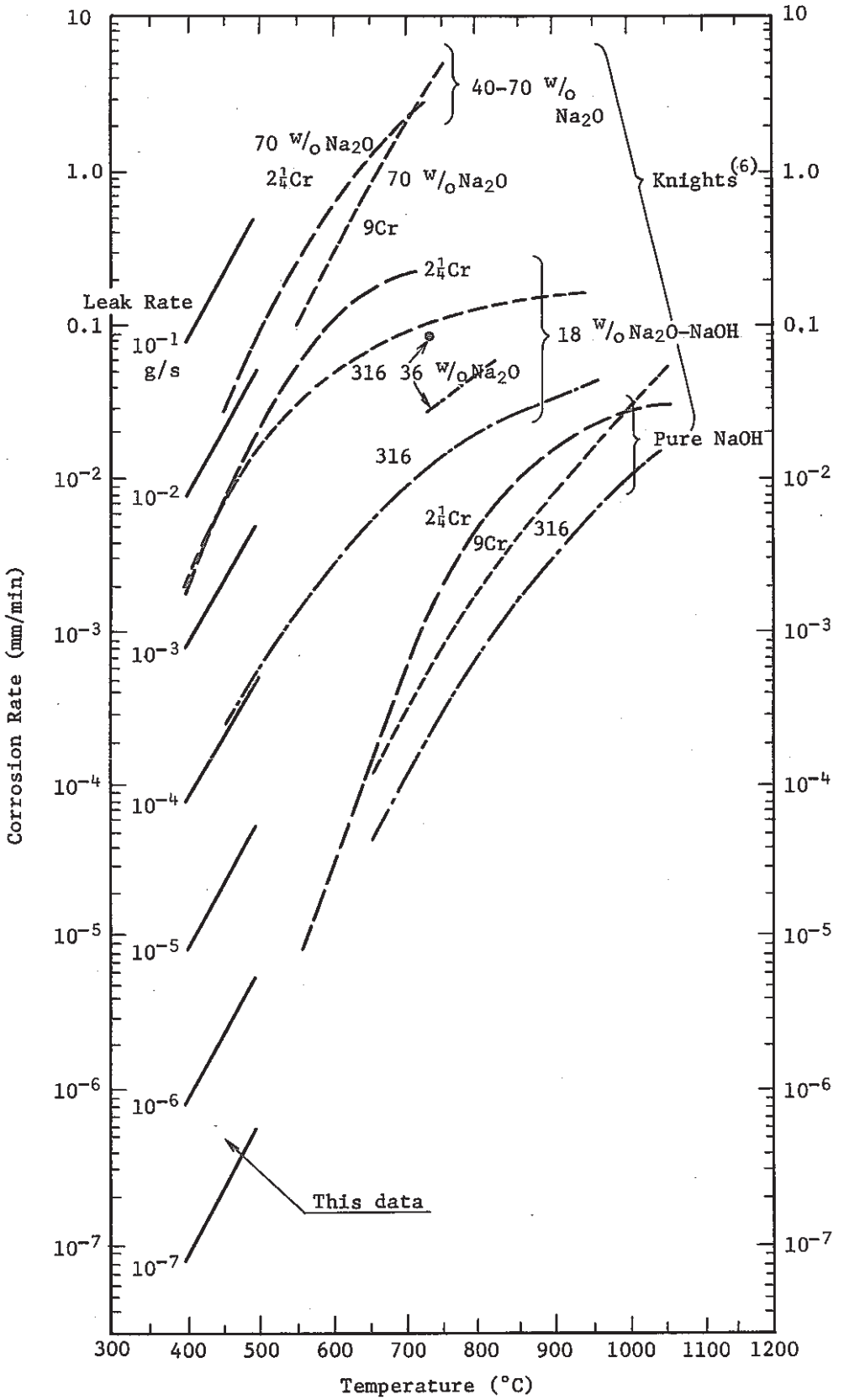

Figure 13 Comparison between the self-wastage rate of Type 321 stainless steel and other corrosion data

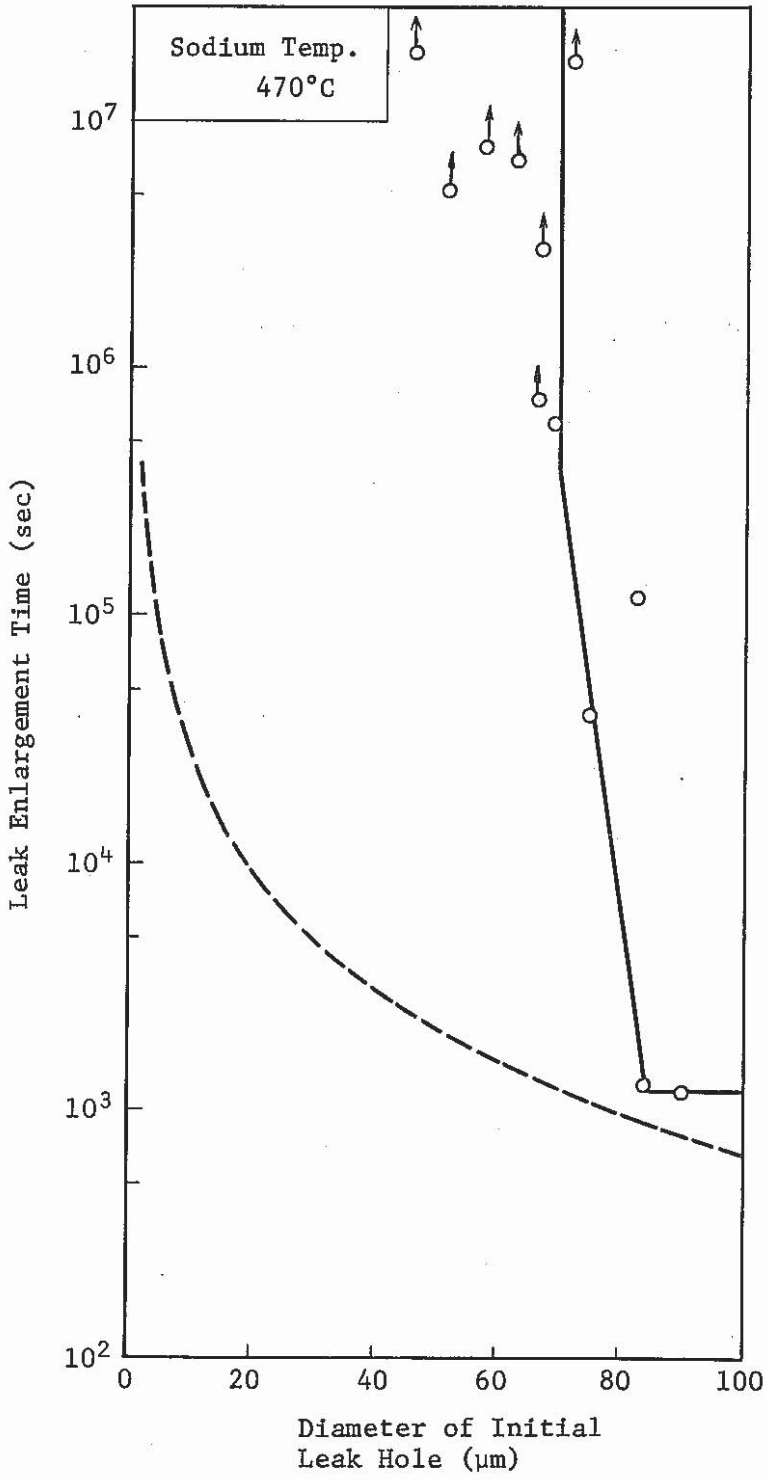

Figure 14 Leak enlargement time on the 2-1/4Cr-1Mo steel micro-leak nozzle

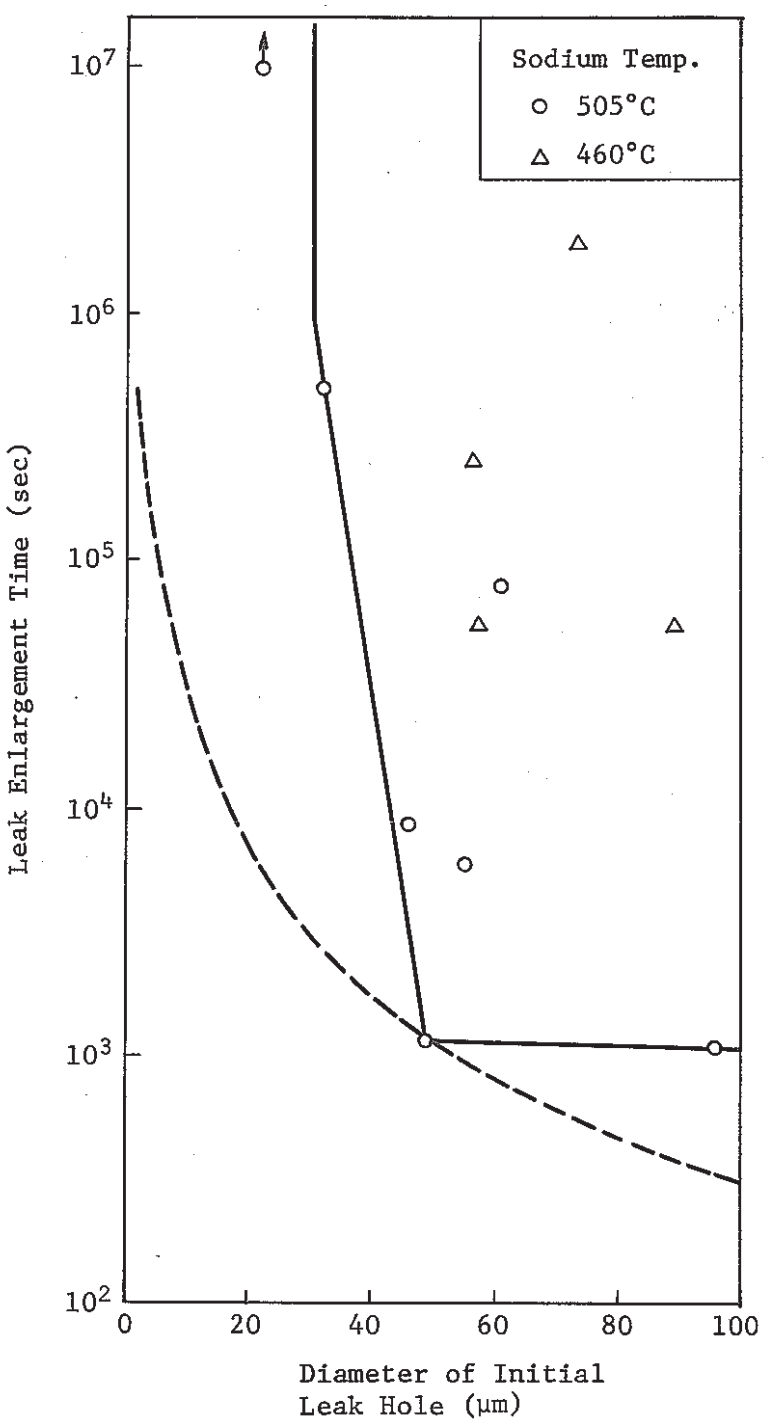

Figure 15 Leak enlargement time on Type 321 stainless steel micro-leak nozzle

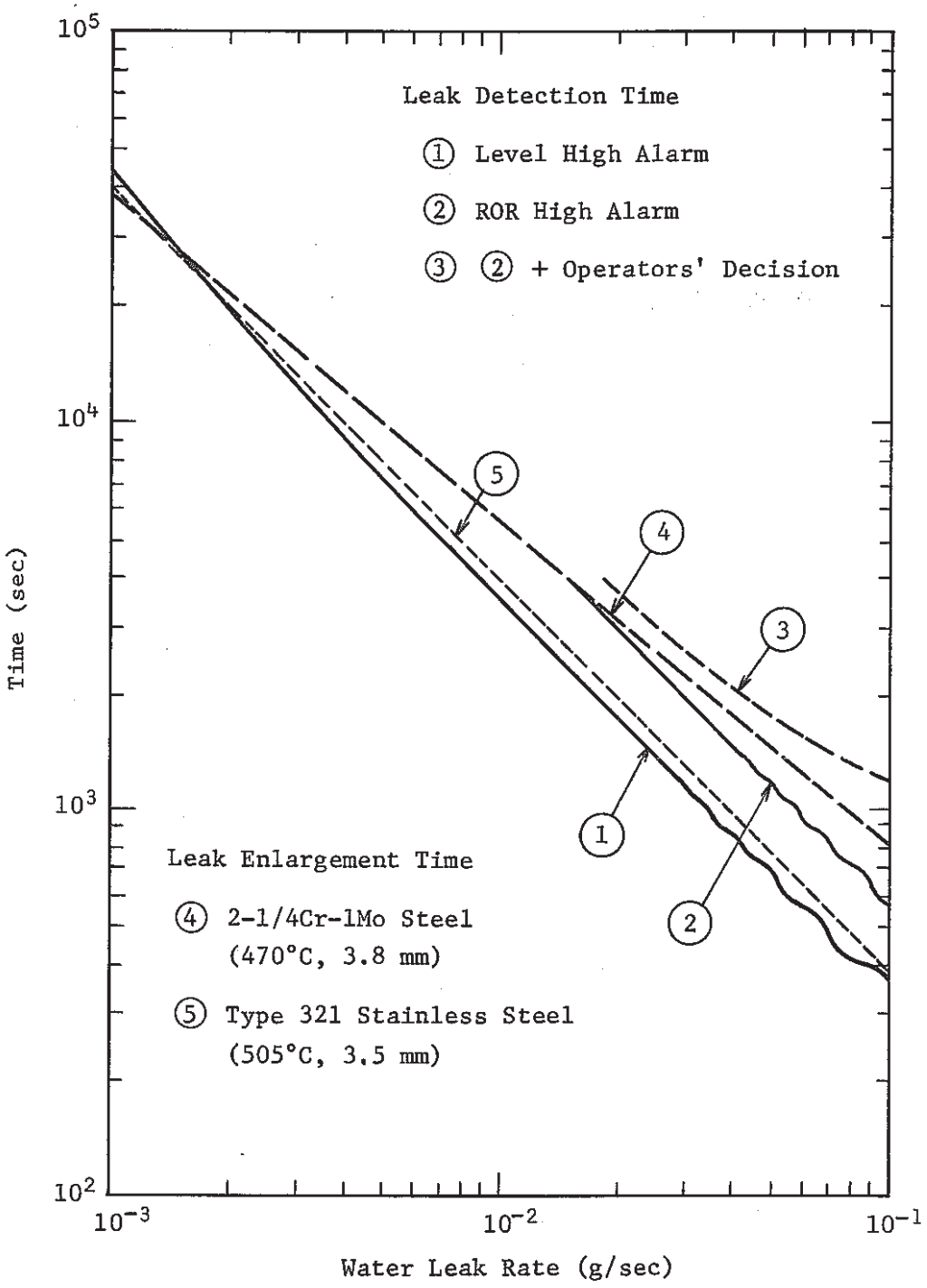

Figure 16 Relation between the leak detection time in the Monju secondary loop and the leak enlargement time due to the self-wastage